RTV Silicones

RTV Number... GO

ALL MG PRODUCTS

Jump to Product Number
Product Number... GO

3M Engineered Fluids
3M Electronic Liquids
Accessories
Adhesives
Brushes
Contact Cleaners
Desoldering Braid
Dusters & Circuit Coolers
Electronic Cleaners
EMI / RFI Shielding
Epoxies
Flux and Flux Remover
Greases & Lubricants
Isopropyl Alcohol
Lead Free Solder
Leaded Solder
Pens
Potting & Encapsulating
Protective Coatings
Prototyping Materials
RTV Silicones
Screen Cleaners
Soldering/desoldering
SpecialtyCleaners
Specialty Products
Swabs
Thermal Management
Thermally Conductive Adhesives
Wipes

RTV Silicones by MOMENTIVE

RoHS COMPLIANT

2-Part Potting/Encapsulating Compound RTV615

STOCKED ITEM

BUY NOW

Primary Characteristics
- **Optically Clear**
- Easily pourable
- Addition cure
- Primer required
- FDA Approved

Use for:
- Solar cell potting
- Optical instruments
- Applications requiring visual identification of potted assemblies
- Food applications

Excellent for potting solar cells for maximum light transmission and electronic assemblies where component identification is desirable. This two part silicone is supplied with a curing agent. Primer required. Cures at room temperature. Has low viscosity allowing easy flow in and around complex parts, providing excellent electrical insualtion and shock resistance. Clarity permits visual inspection foreasy indentification and repair of encapsulated parts. Excellent retention of elastomeric properties at temperatures up to 204°C (400°F). Will cure in deep sections or enclosed assemblies without exotherm and with low shrinkage. Can be used in food contact applications where FDA 21 CFR 177.2600 regulations apply.

Available Sizes

Catalog No.	Description	
RTV615-1P	RTV615 001-KIT (1.0 Lbs-0.454 Kg)	
RTV615-1G	RTV615 010-Pail Kit (10.01 Lbs-4.545 Kg)	
RTV615-5G	RTV615 044-PL BX Kit (44 Lbs-19.976 Kg)	SPECIAL ORDER
RTV615-440LB	RTV615 440-DR PL Kit (440LBS-199.76KG)	SPECIAL ORDER
RTV615B-5G	RTV615B 5GP-Pail (40.0LBS-18.16KG)	SPECIAL ORDER
RTV615A-55G	RTV615A 55G-Drum (400.0LBS-181.60KG)	SPECIAL ORDER

RTV615 requires a primer. Visit our primer guide for details.

Specifications

Use	Adhesive Sealant
Special Feature	High tensile strength Optically Clear
Standards	FDA 21CFR 177.2600
Cross Reference	RTV615
GE Silicone National Stock Number	
5970-00-485-9200	
5970-00-771-7670	
5970-00-988-6125	
5970-00-899-4323	
8030-00-485-9200	
Uncured Properties	
Consistency	Easily pourable
Color	Optical clear
Specific Gravity	1.05
Tack Free Time	4 hours
Cure Through Time	6 - 7 days @ 25°C 15 min @ 150°C

Technical Support for RTV Silicones

1-800-295-2392

M.G. Chemicals Disclaimer for RTV Silicones >

Locate Distributor >

Quick Links

- MSDS
- Catalyst options/MSDS
- Primer options/MSDS
- Specifications
- Spec Sheet
- Available Sizes

Related products:
- RTV103 Black
- RTV108 Translucent
- RTV109 Aluminum

Resources

- Selection Guide
- One Part Chart
- Two Part Chart

Find by Application

- General Purpose
- Aerospace
- Marine
- High Performance Assembly
- Electronics
- Thermal Conductivity
- High Temperature
- Low Temperature

Google

Google Search MG

Useful Temp. Range	-60°C to 205°C (-75°F to 400°F)
Cured Properties - MECHANICAL	
Hardness	44 (Shore A)
Tensile Strength	6.37 MPa (920 psi)
Elongation	120%
Cured Properties - ELECTRICAL	
Volume Resistivity	1.8×10^{15} ohm · cm
Dielectric Strength	19.7 kV/mm
	500 V/mil
Dielectric Constant	2.7 @ 1000 Hz
Cured Properties - THERMAL	
Thermal Conductivity	0.19 W/m · °K
Brittle Point	-60°C (-75°F)
Thermal Expansion	27×10^{-5} (°C)$^{-1}$
Other	
Viscosity (@ 25°C)	4,000 cps
Mix Ratio (by weight)	10 : 1
Pot Life	4 hours
Index of Refraction	1.406

Return to top ^

GE Bayer Silicones

RTV615 and RTV655

Transparent Silicone Rubber Compounds

Product Description

RTV615 and RTV655 silicone rubber compounds are clear liquids, which cure at room temperature to silicone rubber with the addition of curing agents. These two-component products are supplied with curing agent in matched kits, which are designed for use at a convenient 10:1 ratio by weight.

These compounds are clear and colourless but differ in low temperature flexibility. Both are low viscosity, easily pourable liquids with nominal viscosities ranging between 3000 and 7000 mPa·s. RTV655 silicone rubber compound has the capability of remaining flexible at temperatures 55 °C lower than its companion product.

RTV615 and RTV655 silicone rubber compounds are being used for protection of electronic components and assemblies against shock, vibration, moisture, ozone, dust, chemicals, and other environmental hazards by potting or encapsulation of the components and assemblies.

The optical clarity of these silicone rubber compounds suggests evaluation for applications such as potting solar cells for maximum light transmission and electronic assemblies where component identification is necessary or desirable. RTV655 silicone rubber compound is preferred where flexibility at temperatures down to -115 °C is required.

Key Performance Properties

- Convenient 10:1 mixing ratio use in automatic dispensing or hand operations
- Low viscosity allows easy flow in and around complex parts, providing excellent electrical insulation and shock resistance
- Cure rate can be accelerated by heat
- Will cure in deep sections or enclosed assemblies without exotherm and with low shrinkage
- Chemical composition contains no solvents for ease of use on production lines
- Reversion resistance and hydrolytic stability permit use in high humidity environments at elevated temperatures
- Clarity permits visual inspection for easy identification and repair of encapsulated parts
- Retention of elastomeric properties at temperatures up to 200 °C.

Typical Product Data

Uncured Properties		**RTV615A**	**RTV615B**	**RTV655A**	**RTV655B**
Colour		Clear, colourless	Clear, colourless	Clear, colourless	Clear, colourless
Consistency		Easily pourable	Easily pourable	Easily pourable	Easily pourable
Viscosity	mPa·s	4300	-	5700	-
Specific Gravity	g/cm³	1.02	-	1.04	-

Uncured properties with curing agent added		**RTV615**	**RTV655**
Mix ratio		10:1	10:1
Colour		Clear, colourless	Clear, colourless
Consistency		Easily pourable	Easily pourable
Viscosity	mPa·s	4000	5200
Work time @ 25 °C	hrs	4	4

Cured properties		*(Cured 1 hr @ 100 °C)*	
Mechanical		**RTV615**	**RTV655**
Hardness	Shore A	44	45
Tensile strength	MPa	6.5	6.5
Elongation	%	120	120
Shrinkage	%	0.2	0.2
Refractive index		1.406	1.430
Dielectric strength	kV/mm	19.7	19.7
Electrical			
Dielectric constant @ 1 kHz		2.7	2.7
Dissipation factor @ 1 kHz		0.0006	0.0004
Volume resistivity	Ohm · cm	1.8×10^{15}	1.8×10^{15}
Thermal			
Useful temperature range	°C	-60 to 200	-115 to 200
Thermal conductivity	W/m · K	0.2	0.2
Coefficient of expansion	m/m · K	27×10^{-5}	33×10^{-5}
Specific heat	J/g · K	1.3	1.3

Specifications

Typical product data values should not be used as specifications. Assistance and specifications are available by contacting GE Bayer Silicones Technical Service RTV1 and RTV2.

FDA STATUS
RTV615 silicone rubber compound and SS4120 silicone primer may be used in food contact applications where FDA regulations apply.

Instruction for Use

Compatibility

RTV615 and RTV655 silicone rubber compounds will cure in contact with most clean, dry surfaces. However, certain materials, such as butyl and chlorinated rubber, sulphur-containing materials, amines, and certain metal soap-cured RTV silicone rubber compounds, can cause cure inhibition. Cure inhibition is characterized by a gummy appearance of the RTV silicone rubber compound at the interface between it and the substrate.
It is recommended that a sample patch test be performed with RTV615 and RTV655 silicone rubber compounds to determine if a barrier coating or other inhibition-preventing measures are necessary before pouring the material.

Mixing

Select a mixing container 4-5 times larger than the volume of RTV silicone rubber compound to be used. Weigh out ten parts of the A component and one part of the B component. Since RTV615 and RTV655 silicone rubber compounds are kit-matched, work time (or pot life), cure time, and final properties of the cured RTV silicone rubber compound can be assured only if the A component is used with the B component from the same kit.

With clean tools, thoroughly mix the A and B components together, scraping the sides and bottom of the container carefully to produce a homogeneous mixture. When using power mixers, avoid excessive speeds, which could entrap large amounts of air or cause overheating of the mixture, resulting in shorter pot life.

Deaeration

Air entrapped during mixing should be removed to eliminate voids in the cured product. Exposing the material to an absolute pressure of 10-30 mbar can do this. The material will expand, crest, and recede to approximately two minutes after frothing ceases. When using the RTV silicone rubber compound for potting, a deaeration step may be necessary after pouring to avoid capturing air in complex assemblies.
Automatic equipment designed to meter, mix, deaerate, and dispense two-component RTV silicone rubber compounds will add convenience to continuous or large volume operations.

Curing

RTV615 and RTV655 silicone rubber compounds will cure sufficiently in 24 hours at 25 °C to permit handling. To achieve optimum properties an elevated temperature cure or a cure time of 7 days at room temperature is required. The table below illustrates the effect of temperature on cure time:

Temperature	Cure Time*
25 °C	6-7 days
65 °C	4 hrs.
100 °C	1 hr.
125 °C	45 min.
150 °C	15 min.

* Cure times are only approximate. The actual time is affected by the mass of the unit and the time required to reach the desired temperature.

Bonding

These silicone rubber compounds require a primer to bond to non-silicone surfaces.
Thoroughly clean the substrate with a non-oily solvent such as iso-propanol or methyl-ethyl-ketone and allow the primer to air dry for one hour or more. Finally, apply freshly catalyzed RTV silicone rubber compound to the primed surface and cure as recommended. When dry SS4155 silicone primer exhibits a white haze, which will show through RTV615 and RTV655 silicone rubber compounds. If the appearance of the surface to be bonded must be unchanged, SS4120 silicone primer (which dries to an invisible film) may be used.

Handling Safety

Material Safety Data Sheets are available upon request from GE BAYER SILICONES. Similar information for solvents and other chemicals used with the GE Bayer products should be obtained from your supplier. When solvents are used, proper safety precautions must be observed.

Caution

RTV615B and RTV655B curing agents can generate flammable hydrogen gas upon contact with acidic, basic, or oxidizing materials. Such contact should be avoided.

Storage and Warranty Period

The warranted shelf life will be indicated by the 'use before date' on the associated documents with a minimum of 4 months when stored in the original unopened container below 27 °C.

Availability

RTV615 is available as kits in 450g and 4.5 kg cans, 20 kg pails and 200 kg drums.

RTV655 is available in 4.5 kg cans.

RTV 615 A+B - kit (5l-4.54kg)
Crosslinking Agent

1. CHEMICAL PRODUCT AND COMPANY IDENTIFICATION

Manufactured By: **GES Waterford Plant**
260 Hudson River Rd
Waterford NY 12188
Revised: 05/07/2004
Preparer: PRODUCT STEWARDSHIP COMPLIANCE AND STANDARDS
CHEMTREC 1-800-424-9300

Chemical Family/Use: Silicone Elastomer
Formula: Mixture

HMIS

Flammability:	1	Reactivity:	0	Health:	0	Prot. Equipm.:

NFPA

Flammability:	1	Reactivity:	0	Health:	1	Special Haz.:

2. COMPOSITION/INFORMATION ON INGREDIENTS

PRODUCT COMPOSITION	CAS REG NO.	WGT. %
A. HAZARDOUS		
Benzene	71-43-2	0.0001
Toluene	108-88-3	0.5000
B. NON-HAZARDOUS		
VINYLPOLYDIMETHYLSILOXANE	68083-19-2	30 - 60 %
Modified Silica	68988-57-8	30 - 60 %

3. HAZARDS IDENTIFICATION

EMERGENCY OVERVIEW
CAUTION! May cause skin, eye, and respiratory tract irritation. May generate formaldehyde at temperatures greater than 150 C(300 F). See Section 3 of MSDS for details.
Form: liquid Color: Translucent Odor: slight

POTENTIAL HEALTH EFFECTS

INGESTION
None known.

SKIN
Skin contact may cause irritation.

INHALATION
Causes irritation of the mouth, nose, and throat.

EYES
May cause mild eye irritation.

MEDICAL CONDITIONS AGGRAVATED
None known.

SUBCHRONIC (TARGET ORGAN)
None known.

CHRONIC EFFECTS / CARCINOGENICITY
This product or one of its ingredients present 0.1% or more is NOT listed as a carcinogen or suspected carcinogen by NTP, IARC, or OSHA.

ROUTES OF EXPOSURE
dermal; Eyes; Inhalation

OTHER
This product contains methylpolysiloxanes which can generate formaldehyde at approximately 300 degrees Fahrenheit (150'C) and above, in atmospheres which contain oxygen. Formaldehyde is a skin and respiratory sensitizer, eye and throat irritant, acute toxicant, and potential cancer hazard. An MSDS for formaldehyde is available from GE Silicones.

4. FIRST AID MEASURES

INGESTION
Do not induce vomiting. Drink 1 or 2 glasses of water. If symptoms persist, call a physician. Never give anything by mouth to an unconscious person.

SKIN
Wash with soap and water. Get medical attention if irritation or symptoms from Section 3 develop.

INHALATION
If inhaled, remove to fresh air. If not breathing give artificial respiration using a barrier device. If breathing is difficult give oxygen. Get medical attention.

EYES
In case of contact, immediately flush eyes with plenty of water for at least 15 minutes and get medical attention if irritation persists.

NOTE TO PHYSICIAN
None known.

5. FIRE-FIGHTING MEASURES

FLASH POINT: > 121 °C; 249.80 °F
METHOD:
IGNITION TEMPERATURE: NA
FLAMMABLE LIMITS IN AIR - LOWER (%): no data available
FLAMMABLE LIMITS IN AIR - UPPER (%): no data available

SENSITIVITY TO MECHANICAL IMPACT: No

SENSITIVITY TO STATIC DISCHARGE
Sensitivity to static discharge is not expected.

EXTINGUISHING MEDIA
All standard extinguishing agents are suitable.

SPECIAL FIRE FIGHTING PROCEDURES
Firefighters must wear NIOSH/MSHA approved positive pressure self-contained breathing apparatus with full face mask and full protective clothing.

6. ACCIDENTAL RELEASE MEASURES

ACTION TO BE TAKEN IF MATERIAL IS RELEASED OR SPILLED
Wipe, scrape or soak up in an inert material and put in a container for disposal. Wash walking surfaces with detergent and water to reduce slipping hazard. Wear proper protective equipment as specified in the protective equipment section.

7. HANDLING AND STORAGE

STORAGE

PRECAUTIONS TO BE TAKEN IN HANDLING AND STORAGE
Avoid contact with skin and eyes. Keep away from children.

8. EXPOSURE CONTROLS / PERSONAL PROTECTION

ENGINEERING CONTROLS
Eyewash stations; Showers

RESPIRATORY PROTECTION
If exposure limits are exceeded or respiratory irritation is experienced, NIOSH/MSHA approved respiratory protection should be worn. Supplied air respirators may be required for non-routine or emergency situations. Respiratory protection must be provided in accordance with OSHA regulations (see 29CFR 1910.134).

PROTECTIVE GLOVES
rubber gloves

EYE AND FACE PROTECTION
safety glasses with side-shields

OTHER PROTECTIVE EQUIPMENT
Wear suitable protective clothing and eye/face protection.

Exposure Guidelines

Component	CAS RN	Source	Value

Absence of values indicates none found

PEL - OSHA Permissible Exposure Limit; TLV - ACGIH Threshold Limit Value; TWA - Time Weighted Average

OSHA revoked the Final Rule Limits of January 19, 1989 in response to the 11th Circuit Court of Appeals decision (AFL-CIO v. OSHA) effective June 30, 1993. See 29 CFR 1910.1000 (58 FR 35338).

9. PHYSICAL AND CHEMICAL PROPERTIES

BOILING POINT - C & F:	NA
VAPOR PRESSURE (20 C) (MM HG):	Negligible
VAPOR DENSITY (AIR=1):	1.0
FREEZING POINT:	NA
MELTING POINT:	NA
PHYSICAL STATE:	liquid
ODOR:	slight
COLOR:	Translucent
EVAPORATION RATE (BUTYL ACETATE=1):	< 1
SPECIFIC GRAVITY (WATER=1):	ca. 0.99
DENSITY (KG/M3):	ca. 990 KG/M3
ACID / ALKALINITY (MEQ/G):	Unknown
pH:	no data available
VOLATILE ORGANIC CONTENT (VOL):	
SOLUBILITY IN WATER (20 C):	insoluble
SOLUBILITY IN ORGANIC SOLVENT (STATE SOLVENT):	Soluble in toluene
VOC EXCL. H2O & EXEMPTS (G/L):	

10. STABILITY AND REACTIVITY

STABILITY
Stable

HAZARDOUS POLYMERIZATION
Will not occur

HAZARDOUS THERMAL DECOMPOSITION / COMBUSTION PRODUCTS
Carbon monoxide; carbon dioxide (CO2); Silicon dioxide.; formaldehyde

INCOMPATIBILITY (MATERIALS TO AVOID)
None known.

CONDITIONS TO AVOID
None known.

11. TOXICOLOGICAL INFORMATION

ACUTE ORAL
Unknown

ACUTE DERMAL
Unknown

ACUTE INHALATION
Unknown

OTHER
None.

SENSITIZATION
no data available

SKIN IRRITATION
no data available

EYE IRRITATION
no data available

MUTAGENICITY
Unknown

12. ECOLOGICAL INFORMATION

ECOTOXICOLOGY
no data available

CHEMICAL FATE
no data available

DISTRIBUTION
no data available

13. DISPOSAL CONSIDERATIONS

DISPOSAL METHOD
Disposal should be made in accordance with federal, state and local regulations.

14. TRANSPORT INFORMATION

Not Regulated if Section is Blank

15. REGULATORY INFORMATION

US Regulatory Information

CERCLA

PRODUCT COMPOSITION	Chemical	CERCLA Reportable Quantity

CLEAN AIR ACT

CLEAN WATER ACT

SARA SECTION 302

SARA (311,312) HAZARD CLASS
None.

SARA (313) CHEMICALS

Canadian Regulatory Information

WHMIS HAZARD CLASS
NON-CONTROLLED

Other

SCHDLE B/HTSUS:

ECCN:

CALIFORNIA PROPOSITION 65

Warning! This product contains a chemical known to the State of California to cause cancer, birth defects or other reproductive harm
71-43-2, Benzene. 108-88-3, Toluene.

16. OTHER INFORMATION

OTHER

These data are offered in good faith as typical values and not as product specifications. No warranty, either expressed or implied, is made. The recommended industrial hygiene and safe handling procedures are believed to be generally applicable. However, each user should review these recommendations in the specific context of the intended use and determine whether they are appropriate....., C = ceiling limit NEGL = negligible EST = estimated NF = none found NA = not applicable UNKN = unknown NE = none established REC = recommended ND = none determined V = recommended by vendor By-product = reaction by-product; TSCA inventory status not required under 40 CFR part 720.30(h-2) SKN = skin TS = trade secret R = recommended MST = mist ST = short term exposure limit NT = not tested ppm = parts per million ppb = parts per billion .....

Fibre gratings written through the coating at 244nm and 248nm

Laurence Reekie, Lu Chao* and Morten Ibsen

Abstract

Fibre Bragg gratings have been written through the fibre coating using 244nm frequency-doubled Ar^+-ion 248nm KrF excimer lasers for the first time. A standard off-the-shelf coating was used, and 92% reflectivity gratings were obtained with an index change of 2.4×10^{-4}.

Introduction

Fibre Bragg gratings are widely used in the fields of optical fibre communication and fibre sensor systems. In the normal process of fibre grating fabrication, all coatings must be stripped off before the grating can be written and, in order to preserve the mechanical strength of the fibre, it must be re-coated soon after the grating is written. This method is both time consuming and has the potential of reducing the fibre strength due to exposure of the bare fibre to the air. To solve the problem, a number of solutions have been proposed. These include using a specially developed UV-transparent polymer coating [1], writing the grating using near UV light around 330nm instead of at more conventional wavelengths [2], writing on-line as the fibre is being pulled [3] and using a specially developed coating which can be removed thermally then immediately re-coating in an automated production system [4]. The polymer used in [1], although it has a lower absorption than the normal UV-curable polymer coating, still has a strong absorption below 260nm. This increases the grating writing time and reduces the mechanical strength of the fibre when higher UV exposure power is used [5]. In [2], a specially developed phase mask is needed in order to operate at the non-standard wavelength. In addition, care is also required to control the average laser power in order to reduce damage to the coating. On-line production of fibre gratings [3] is limited to the manufacture of gratings which can be made with a single laser pulse. The method proposed in [4], although attractive, requires both a special coating and an automatic production system. The thermally strippable coating also has a low heat resistance in many applications. In this letter, we demonstrate for the first time writing of a fibre grating through a normal off-the-shelf fibre coating using wavelengths of 244 and 248nm. We show that the scheme is both easy and cost effective.

Experiment and results

The coating we used is General Electric RTV 615 silicone rubber. This coating is thermally curable and thus does not require a UV absorbing photoinitiator. With a normal specified useful temperature range of –60°C to 204°C, the coating has a better thermal tolerance than standard UV curable polymer coating. This is an important advantage in many applications. To determine the absorption of the material in the UV region, a 150μm thick film of cured silicone rubber was formed between

Optoelectronics Research Centre, University Southampton, Southampton, SO17 1BJ, U.K.
Tel : +44 1703 593186, Fax: +44 1703 593149. Email: lr@orc.soton.ac.uk

**Permanent address: School of Electrical and Electronic Engineering, Nanyang Technological University, Singapore 639798*

two silica plates. The absorption characteristics of the coating as measured using a spectrophotometer is shown in Figure 1. A silica plate was used as the reference to improve the

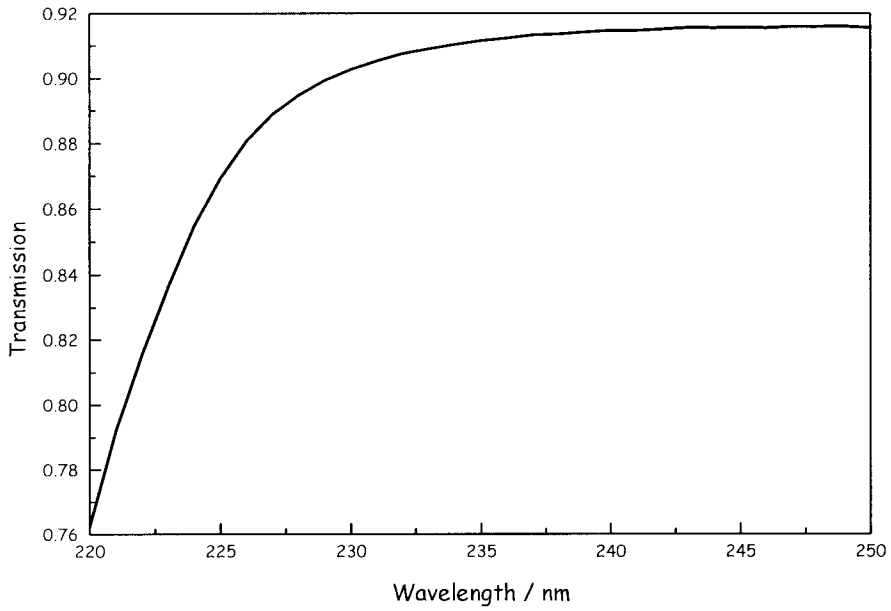

Figure 1: UV transmission characteristics of 150μm thick film of silicone rubber RTV 615.

measurement accuracy. The result clearly indicates a transmission of almost 92% at a wavelength of 248nm. This low UV absorption suggests the possibility of Bragg grating writing through the silicone

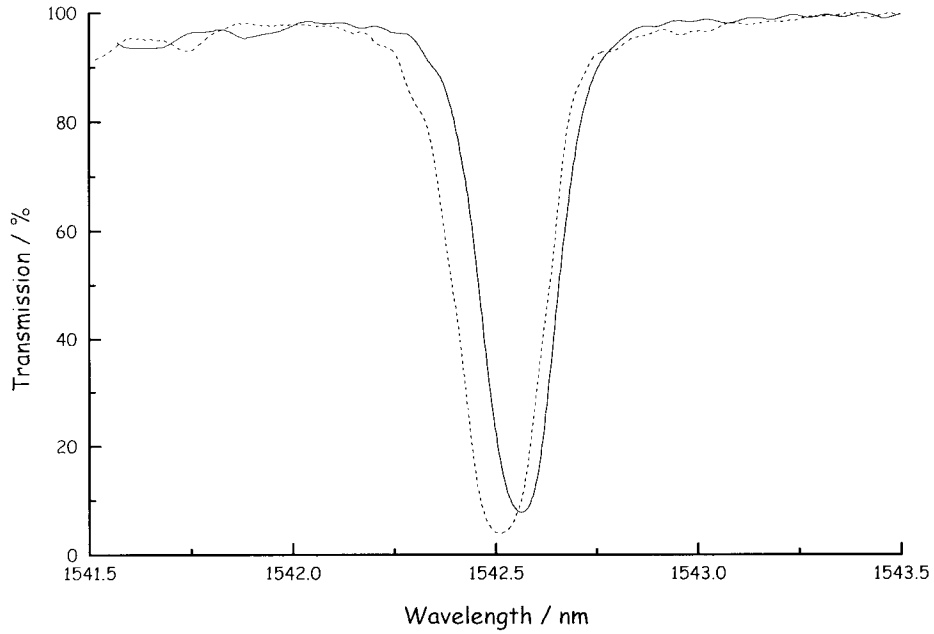

Figure 2: Transmission spectrum of Bragg grating written in coated (solid line) and un-coated (dotted line) fibre.

rubber coating using either a frequency-doubled Ar^+-ion laser at 244nm or a KrF excimer laser at 248nm. To verify this, we coated a photosensitive boron co-doped silica/germania photosensitive

fibre (NA=0.12, $\lambda_{cut\text{-}off}$=1050nm, diameter=125μm) with the silicone rubber coating. The average coating thickness was 60μm, similar to a normal fibre coating. Grating inscription was initially carried out using a 248nm excimer laser and a 1540nm phase mask optimised for 248nm operation. A 1cm long grating was produced by scanning a 3mm wide beam over a section of the coated fibre, each individual part of the fibre receiving an exposure of 3 minutes at 20Hz. The spectrum was monitored using an optical spectrum analyser and 1.55μm LED. The individual pulse fluence was set at 64mJ/cm^2. A grating with a reflectivity of 92% was obtained, limited by the resolution of the optical spectrum analyser (approximately 0.1nm), corresponding to an index change of 2.4×10^{-4}, and the resulting grating is shown in figure 2. For comparison, we also stripped off the coating and exposed the fibre under identical conditions, and this grating is also shown in figure 2. The almost identical result suggests that the effect of writing through the coating is almost negligible.

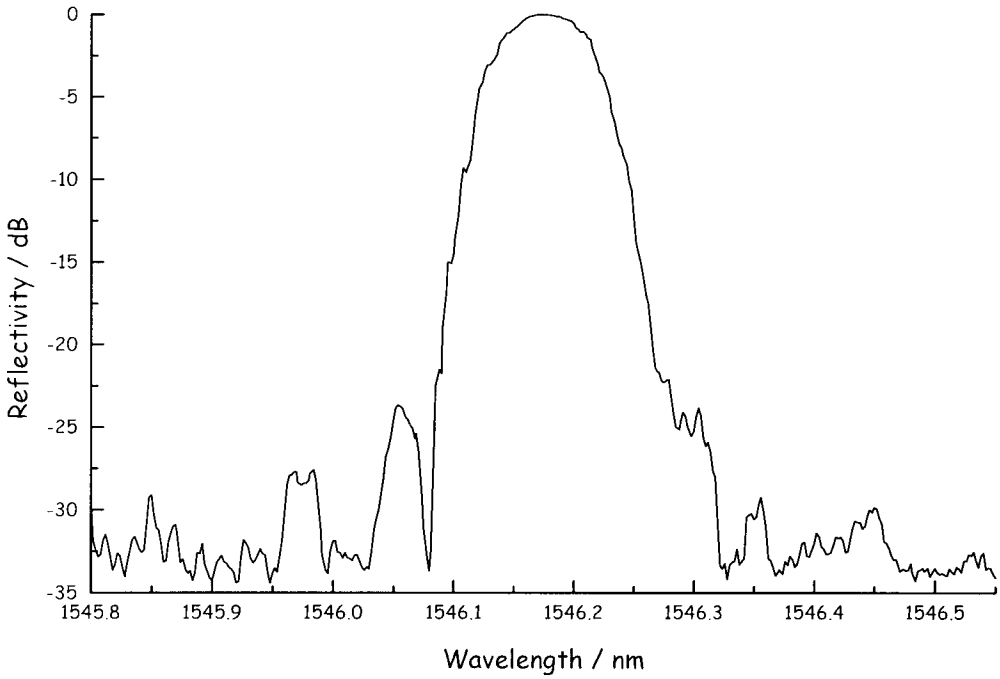

Figure 3: Transmission spectrum of Blackman apodised Bragg grating written in coated fibre.

In order to test for possible coating-induced thermal effects on grating uniformity, a 25mm long Blackmann apodised grating was written through the coating at 244nm using a frequency-doubled Ar^+-ion laser in the same fibre, and the reflection characteristic is shown in figure 3. The intensity was 2.2kW/cm^2 with a total fluence of 1kJ/cm^2. It can be seen that most of the reflected light outside of the central peak is >30dB down on the peak reflectivity, showing excellent grating uniformity. The index change obtained was 1.0×10^{-4}.

To verify the heat resistance of the coating we have placed a fibre with the silicone rubber coating together with a fibre coated with UV curable polymer on a hot plate with a temperature of 300°C for 3 minutes. A visible darkening of the polymer was observed. However, the effect on the silicone rubber coated fibre was negligible.

Conclusions

In this letter we have demonstrated for the first time the ability to write fibre gratings through standard fibre coating at 244 and 248nm. We have shown that the scheme is not only simple but also

has several advantages over other previously demonstrated techniques. The ability to write through the fibre coating at these wavelengths is most useful since it will significantly simplify the grating writing process, particularly for long arrays of gratings as required for fibre sensors.. The better heat resistance not only means that it can be used in many different applications but also allows the grating to be annealed if there is such a requirement, *e.g.* after hydrogen loading. One potential drawback is the refractive index of the coating which, at 1.406, does not allow for complete stripping of cladding modes. Further work is required to eliminate this problem.

Acknowledgements

The financial support of the Tan Chin Tuan exchange fellowship of the Nanyang Technological University to allow Lu Chao to be attached to the ORC and EPSRC funding for the project is acknowledged. We would also like to acknowledge useful discussions with Dr. Eleanor Tarbox and Dr. David Richardson and the assistance of Michael Langton in coating the fibre.

References

1. Espindola, R.P., Atkins, R.M., Simoff, D.A., Nelson, K.T., and Paczkowski, M.A.: 'Fibre Bragg Grating Written Through a Fibre Coating', OFC'97 Tech. Dig., 1997, Postdeadline paper PD-4.

2. Starodubov, D.S., Grubsky, V., and Feinberg J.: 'Efficient Bragg grating fabrication in a fibre through its polymer jacket using near-UV light', Electron. Lett. 1997, **33**, pp.1331-1333.

3. Dong, L., Archambault, J.-L., Reekie, L., Russell, P.St.J. and Payne, D.N.: 'Single pulse Bragg gratings written during fibre drawing', Electron. Lett., 1993, **29**, pp.1577-1578.

4. Singh, H., Cronk, B., Speaks, S. and Novak, J.: 'Automated In-Line Production of Fibre Bragg Grating Using Special Coatings', Proc. ECOC 97, IEE Conference Publication No. 488. pp.173-176.

5. Imamura, K., Nakai, T., Moriura, K., Sudo, Y., and Imada, Y., 'Mechanical Strength Characteristics of Tin-Codoped Germanosilicate Fibre Bragg Grating by Writing Through UV-Transparent Coating ' Electron. Lett. 1998, **34**, pp.1016-1017.

Solar Energy Materials & Solar Cells 94 (2010) 246–253

Contents lists available at ScienceDirect

Solar Energy Materials & Solar Cells

journal homepage: www.elsevier.com/locate/solmat

Ultraviolet light test and evaluation methods for encapsulants of photovoltaic modules

Michael D. Kempe*

National Renewable Energy Laboratory, 1617 Cole Blvd., Golden, CO 80401, USA

ARTICLE INFO

Article history:
Received 18 May 2009
Received in revised form
11 September 2009
Accepted 15 September 2009
Available online 14 November 2009

Keywords:
Photovoltaic
Adhesion
Ultraviolet
Degradation
Cerium
Glass

ABSTRACT

Photovoltaic (PV) modules are exposed to harsh conditions of heat, humidity, high voltage, mechanical stress, thermal cycling, and ultraviolet (UV) radiation. The current qualification tests (*e.g.* IEC 61215) do not require UV exposure sufficient to evaluate a lifespan of 20 years or more. Methods to quickly evaluate the UV durability of photovoltaic materials are needed. The initial performance and cost of encapsulant materials must be taken into account, but equally important is their ability to maintain adhesion and transmissivity under UV exposure. This can be evaluated under highly accelerated conditions with light from a xenon arc lamp using glass that transmits more UV radiation than a module would normally see. The use of highly UV transmissive glass (no Ce to block UV-B radiation) results in a UV dose that is about 3.8 times greater with regard to adhesion than a Ce-containing glass. With this configuration, the effect of 20 years of exposure, as compared with the use of UV-B blocking glass, can be simulated in just over 6 months using standard commercial accelerated stress chambers. This also indicates that the use of non-UV blocking glass may significantly reduce the long-term adhesive stability of PV materials.

1. Introduction

Polymeric encapsulant materials are used in photovoltaic (PV) modules to provide electrical insulation and to protect modules from mechanical damage and environmental corrosion. The PV module qualification tests (such as IEC 61215 [1]) are designed to provide minimum standards for module durability and to demonstrate a degree of safety in the production of electricity [2–4]. The specific effects of these highly accelerated stress tests vary significantly from manufacturer to manufacturer and even more so among different PV technologies [5,6]. These tests alone do not necessarily predict the long-term stability of a module design; their intent is to provide reasonable assurance that a PV panel may perform reliably for a long period of time.

Because of the extreme difficulty of exposing production modules to concentrated light sources, the UV exposure required by these tests corresponds to an equivalent field exposure of several months to 1.5 years rather than the desired service life of 20–30 years. The IEC qualification tests 61215, 61646, and 61730-2, [1,7,8] include a "UV Preconditioning Test" only. Here modules are held at 60 ± 5 °C and subjected to 15 kWh/m^2 between 280 and 385 nm with at least 5 kWh/m^2 between 280 and 320 nm. For comparison the AM 1.5 spectrum [9] contains 35.3 W/m^2 and 1.52 W/m^2 in these ranges, respectively. To achieve the necessary irradiation for the IEC tests using a continuous (indoor) AM 1.5 spectrum it would take 17.7 days for the 280–385 nm range and 137 days for the 280–320 nm range. Because the AM 1.5 spectrum has a total of 1000 W/m^2 and a typical outdoor day/night average is about 250 W/m^2, depending on the location, another factor of 4 is necessary to compare chamber exposure to outdoor exposure [10]. For a typical location, the IEC UV exposure therefore corresponds to a real-time exposure of about 70 days for 280–385 nm and about 500 days for 280–320 nm range. Similarly, IEC 62108 requires a "UV Conditioning Test" consisting of 50 kWh/m^2 below 400 nm. This is equivalent to about 180 days real-time exposure. The existing qualification tests do not nearly provide assurance that a PV module will withstand 20 or more years of UV radiation. These tests are only designed to provide minimum standards for PV panel construction.

Obtaining a 20 year UV dose on a full-size module would be expensive and time consuming. If one were to construct a large room capable of continuously exposing full-size modules to 5 UV suns of radiation, it would still take a year to do so. Obtaining this level of exposure on such a large scale for such long periods of time is undesirable as part of a qualification test.

Alternatively one can evaluate small samples of materials and/or minimodules constructed in a similar manner to a full-size module. With the exception of the Staebler Wronski effect in amorphous Si and similar transient effects in copper indium gallium selenide-based PV cells [11–13], the UV radiation

* Tel.: +1 303 384 6325.
E-mail address: Michael.Kempe@NREL.gov

0927-0248/$ - see front matter © 2009 Elsevier B.V. All rights reserved.
doi:10.1016/j.solmat.2009.09.009

principally acts to degrade the polymeric materials used in PV modules. This degradation ultimately results in polymer embrittlement, delamination and/or discoloration (yellowing) [14]. The work here discusses methods for quickly evaluating polymeric encapsulants for use in PV modules, including the wavelength sensitivity to UV radiation.

2. Experimental

Lap shear tests were conducted as outlined previously by Kempe et al. [15] using an Instron Test Unit (model 1122/5500R). Two 5.61-mm-thick 7.6×7.6 cm glass pieces were used to construct the test specimens. The polymer under test was applied to an approximately 19×19 mm area at a thickness of about 0.5 mm, similar to what is typically used in a PV module.

UV exposure (60 °C/60% RH and 2.5 UV suns) was obtained using an Atlas Ci4000 Weather-Ometer with a light intensity of 114 W/m^2 between 300 and 400 nm using a type "S" borosilicate inner and outer filter. The black panel standard temperature was maintained at 100 ± 7 °C resulting in a temperature of 70–80 °C for the transparent glass lap shear samples.

Yellowness index measurements were made using a Hunter-Lab Ultra Scan spectrocolorimeter. The 1931 calculation standard was used with the D65 spectrum as the illuminant [16,17].

All polymeric samples obtained from outside manufacturers were used as received.

The optical transmittance of polymeric encapsulant materials were measured by curing thick sections of polymer between two pieces of 3.18 mm AFG Krystal Klear glass using rubber "O" rings as spacers. The glass samples obtained here contain trace amount of Ce to reduce UV transmittance. The percent transmittance [$T(\lambda)$] through these samples was measured using a Lambda 9 UV–vis spectrophotometer equipped with an integrating sphere. The polymer thickness was varied between 1.5 and 5.5 mm for each sample and the solar and quantum efficiency weighted transmittance (T_{SW}) was calculated as

$$T_{SW} = \frac{\int T(\lambda) I(\lambda) \lambda QE(\lambda) d\lambda}{\int I(\lambda) \lambda QE(\lambda) d\lambda} \quad (1)$$

Here, $I(\lambda)$ is the AM 1.5 global irradiance [9] in units of W/m^2/nm and $QE(\lambda)$ is the quantum efficiency of a PV cell. Both the top and the bottom integrand were multiplied by the wavelength to yield values related to the photon density, which more closely correlates to the current and energy producing potential of light.

The normal incidence transmittance, T, through a thick plate can be described by Eqs. (2) and (3) where the refractive index of the surrounding medium is assumed to be 1, t is the plate thickness, α is the material absorptivity, k is the extinction coefficient, n is the real component of the refractive index, and $\alpha = 4\pi k/\lambda$,

$$T = \frac{(1 - r_i)^2 e^{-t\alpha}}{1 - r_i^2 e^{-2t\alpha}} \quad (2)$$

$$r_i = \frac{(1-n)^2 + k^2}{(1+n)^2 + k^2} \quad (3)$$

For polymer samples laminated between two glass plates, the reflection at the interface between polymer and glass is at most approximately 0.17% ($n \sim 1.4$ for silicone and $n \sim 1.52$ for glass). For hydrocarbon-based polymers ($n \sim 1.48$) this reflection would be about 0.018%. For the purpose of these measurements this reflection can be ignored yielding

$$T = \frac{(1 - r_{i,g})^2 e^{-(t_g \alpha_g + t_p \alpha_p)}}{1 - r_{i,g}^2 e^{-2(t_g \alpha_g + t_p \alpha_p)}} \quad (4)$$

for the transmittance, where the subscripts p and g indicate properties for the polymer and glass, respectively. Here t_g refers to the sum total thickness of the two pieces of glass and $r_{i,g}$ is determined using Eq. (3) with values for glass. For these samples $r_{i,g}^2 \ll 1$ and absorption in the polymer layer on multiple reflections can be ignored in the denominator of Eq. (4) resulting in Eq. (5).

$$T = \frac{(1 - r_{i,g})^2 e^{-t_g \alpha_g}}{1 - r_{i,g}^2 e^{-2t_g \alpha_g}} e^{-(t_p \alpha_p)} = T_{glass} e^{-(t_p \alpha_p)} \quad (5)$$

Here T_{glass} is the transmittance through a piece of plate glass with thickness t_g. For these measurements T_{glass} was measured as the transmittance through 6.35 mm Krystal Klear glass.

3. Results

3.1. Light transmittance

In addition to mechanically holding a module together, encapsulant materials used on the front side of a PV device must provide good optical coupling for the maximum transmittance of incident photons. To enable evaluation of candidate encapsulant materials, the transmittance of glass and glass/encapsulant/glass laminates was measured and weighted against the solar spectrum and the quantum efficiency of a representative x-Si solar cell (obtained as an average of 8 different cells), Eq. (1). Using these averages in Eq. (5), a solar and quantum efficiency averaged photon absorptivity was obtained (Table 1). With this, the total transmittance to a hypothetical cell through a 3.18 mm piece of glass and through 0.45 mm of encapsulant was estimated as

$$T_{cell} = \frac{(100 + T_{glass})}{2} e^{-(t_p \alpha_p)} \quad (6)$$

This may slightly over estimate the light because T_{glass} includes light from multiple reflections at the air to glass interface; however, the cell to polymer interface will likewise cause multiple reflections; therefore Eq. (6) provides a reasonable estimate. The light that reaches the cell will then be absorbed by the cell as governed by the cell optics and quantum efficiency. This analysis illustrates that despite the large differences in absorptivity, the actual lost power due to photon absorption is not high. Thus, improvements in transmittance over EVA are not expected to produce extremely large improvements in performance.

3.2. Lap shear measurements

Lap shear samples of EVA were made using low Fe glass both with Ce (6.35 mm-thick-Krystal Klear) and without Ce (1990s vintage 5.61-mm-thick PPG Starphire [18]) to evaluate the effect of enhanced UV transmittance on the adhesion of EVA, Fig. 1 [19–21]. The presence and absence of Ce in these glasses was verified using time of flight secondary ion mass spectroscopy [15]. The transmittance of UV light through some sample glasses is shown in Fig. 1 before and after solarization for several hundred hours at 2.5 UV suns in an Atlas Ci4000 Weather-Ometer® [22,23]. The UV-B region extends from 290 to 320 nm and is the region of the solar spectrum typically causing the most damage to hydrocarbon-based polymeric materials. Here we see that the addition of minute amounts of Ce to the glass dramatically reduces the transmittance of UV-B radiation and that solarization of the glass extends this absorption to even longer wavelengths [22].

The effect of increased UV-B transmittance on the adhesion of EVA was evaluated using glass lap shear samples exposed to 2.5

Table 1
AM 1.5 [9] Solar photon-weighted optical density determined from transmittance measurements through polymer samples of various thickness (1.5–5.5 mm) sandwiched between two pieces of 3.18-mm-thick Krystal Klear glass. α calculated according to Eq. (5).

Encapsulant	AM 1.5 solar photon and Si QE weighted absorptivity (1/mm)	Transmission to cells through 3.18 mm glass and 0.45 mm encapsulant (%)	Comments
GE RTV615	0.000 ± 0.003	94.8 ± 0.3	PDMS, addition Cure
Dow Corning sylgard 184	0.002 ± 0.004	94.7 ± 0.3	PDMS, addition cure
Dow Corning 527	0.004 ± 0.003	94.7 ± 0.3	PDMS gel, addition cure
Polyvinyl butyral	0.011 ± 0.005	94.3 ± 0.4	
EVA 0.012 ± 0.005 94.3 ± 0.4			
Thermoplastic polyurethane	0.024 ± 0.004	93.8 ± 0.3	
NREL experimental	0.027 ± 0.006	93.7 ± 0.4	Poly α-olefin copolymer
Thermoplastic ionomer #1	0.049 ± 0.007	92.7 ± 0.4	Copolymer of ethylene and methacrylic acid
DC 1199 SSL	0.064 ± 0.004	92.1 ± 0.3	PDMS, one part neutral condensation cure
DC 700	0.068 ± 0.004	92.0 ± 0.3	PDMS, acetic acid condensation cure
Thermoplastic ionomer #2	0.149 ± 0.007	88.7 ± 0.4	Copolymer of ethylene and methacrylic acid

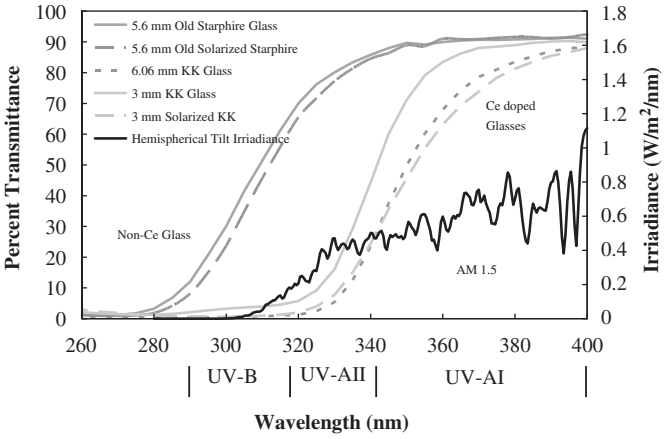

Fig. 1. UV light transmittance through a variety of glass samples plotted with the AM 1.5 spectrum for comparison. Samples labeled "solarized" had been exposed to 114 W/m^2 (300 nm to 400 nm) in a Ci4000 Weather-Ometer® at 60 °C and 60% RH.

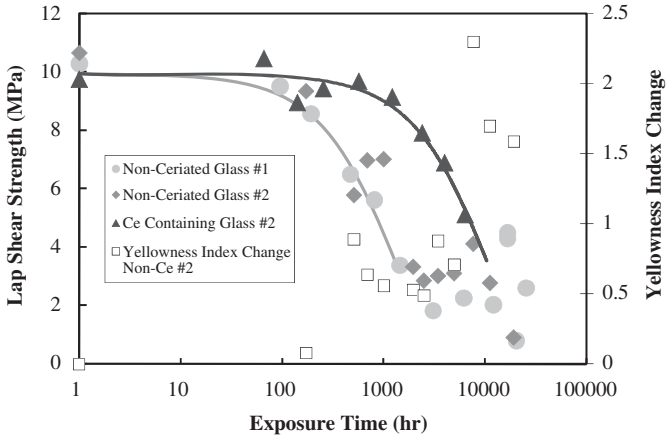

Fig. 2. Lap shear strength and yellowness index change of EVA after exposure to 60 °C/60% RH/2.5 UV suns. EVA was obtained commercially and was formulated specifically for use in PV modules. Samples #1 and #2 refer to slightly different formulations.

UV suns. The fit lines in Fig. 2 are exponential decay curves offset from each other on the time axis by a factor of 8. This fit is empirical in nature and valid only for the initial changes in adhesion. The degradation of lap shear strength for the Ce-doped glass initially dropped to values between 2 and 4 MPa where it remained for about 20,000 h. Once the lap shear strength began to drop, failure was typically around 80–90% on the side facing the UV lamp indicating that the UV light was responsible for loss in adhesion.

Failure almost always occurred by an adhesive mode (i.e. at the glass to polymer interface). The only exception was for the non-ceriated glass sample #1 at 16,700 h which failed about 25% cohesively and the same material at 25,000 h which failed about 50% cohesively. In this case, these samples had noticeably yellowed and shrunk. Originally the samples were about 19×19 mm but had shrunk to about 17×17 mm. This sample appears to have depolymerized under this extreme stress condition. However, this depolymerization, which increases the tack, and the incorporation of oxygen which makes the material more polar, actually improves the adhesion of this material. In subsequent measurements, the amount of depolymerization was much more pronounced and the adhesive strength dropped. In contrast, the non-ceriated glass #2 sample failed adhesively at 19,000 h exposure and did not show any signs of depolymerization. This demonstrates the effects of variations in formulations #1 and #2 on the degradation of a polymer film.

For each of the EVA #2 samples exposed behind the non-ceriated glass, the yellowness index was measured just prior to lap shear testing, Fig. 2. Here one can see that the loss in adhesion correlates with an increase in yellowness. It is not until longer exposure times ($\sim$7500 h) that significant discoloration began to appear. However, these changes in yellowness are relatively small [24,25] and do not correspond to large drops in transmittance. This indicates that a well-formulated EVA film can withstand long exposure and is likely to begin to mechanically degrade before significant yellowing will occur [25].

3.3. UV transmittance to polymer/glass interface

When EVA is formulated for use in PV applications a UV absorber is added to reduce degradation. The transmittance of UV radiation through unformulated EVA, Ce-containing glass, and a glass/EVA/glass sample is shown in Fig. 3 to illustrate the effect of UV absorbers in EVA formulations. Exposure to UV radiation causes deadhesion preferentially on the glass/EVA interface facing the light source as the UV light at the opposite interface is attenuated by the EVA film. Because of this, it is useful to

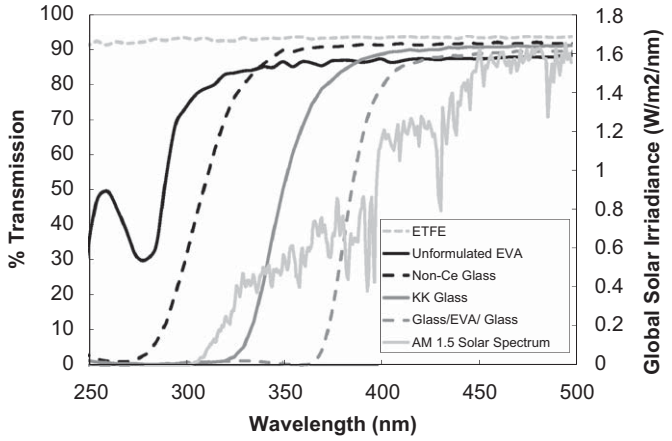

Fig. 3. UV transmittance of PV materials. The "Unformulated EVA" film contains 0.4% BHT (2,6-di-tert-butyl-4-methylphenol) as an antioxidant and is 1.17 mm thick. The "Glass/EVA /Glass" sample was constructed using two 3.18-mm-thick Krystal Klear glass samples and 1.57-mm-thick EVA. "KK glass" is 6.34 mm thick and contains Ce. The non-Ce Glass was 5.61 mm thick. The polyethylene-tetrafluoroetylene (ETFE) was 0.038 mm thick.

quantitatively understand the spectral distribution of light at the glass to EVA interface.

For the lap shear samples in this work, the difference in refractive index between the glass and the polymer is small, so the reflection at this interface is negligible. Therefore, the amount of UV radiation reaching this interface, $I_{E/G}(\lambda)$, is equal to the lamp irradiance, I_{Lamp}, reduced by reflection at the glass-to-air interface, Eq. (3), and by the absorption from a single pass through the glass to the polymer/glass interface

$$I_{E/G}(\lambda) = I_{Lamp}\frac{(1-n_g)^2+k_g^2}{(1+n_g)^2+k_g^2}e^{(4\pi k_p/\lambda)t} \tag{7}$$

Here the subscripts g and p refer to glass and polymer properties respectively. Because the Weather-Ometer simulates natural sunlight while controlling the light between 300 and 400 nm, values for AM 1.5 can be used as an approximation for I_{Lamp}. According to Rubin [26] the real component of the refractive index for typical soda lime glasses can be approximated within $\pm 1\%$ by

$$n = 1.5130 - 0.003169\lambda^2 + \frac{0.003962}{\lambda^2} \tag{8}$$

With these estimates for n_g and the transmittance of light through a sheet of glass after solarization, values of k_g for the glass samples were estimated on a wavelength by wavelength basis using Eqs. (2) and (3) (solved numerically using a VisualBasic™ script in Excel™). From this, the irradiance at the glass to polymer interface, Fig. 4, of the lap shear samples using the different glasses was estimated using Eq. (7).

3.4. Wavelength sensitivity estimates

An action spectrum describes the effectiveness of incoming photons (as a function of wavelength) for producing a specified type of damage. For exposure to a specific spectrum of photons, $\sim I(\lambda)\lambda$, the activation spectrum describes the relative damage as a function of wavelength. The activation spectrum is the mathematical convolution of the action spectrum and source-specific incident irradiance.

Unless there are specific absorption bands in the region of interest, the action spectrum of the incoming photons typically varies exponentially [27,28] with wavelength ($\sim e^{-B\lambda}$) for polymeric materials. With this approximation, the activation

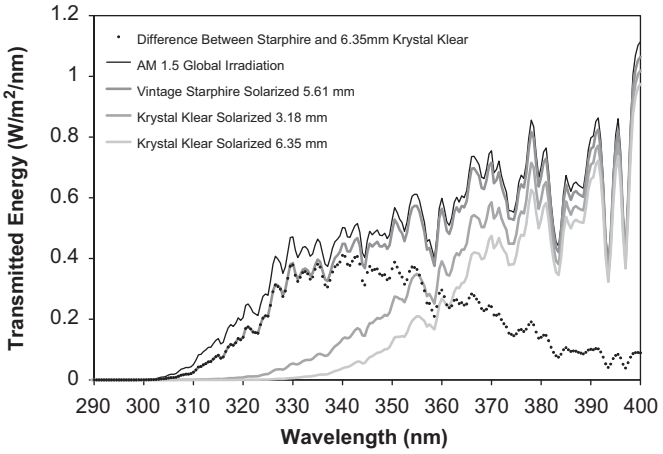

Fig. 4. Estimated irradiance at the glass/EVA interface.

spectrum [$E(\lambda)$] is given by

$$E(\lambda) \sim I(\lambda)\lambda e^{-B\lambda} \tag{9}$$

and the effective UV dose (D) can be estimated as

$$D \sim \int I(\lambda)\lambda e^{-B\lambda} d\lambda \tag{10}$$

where $I(\lambda)$ is the radiant energy in (W/m^2/nm), λ is the wavelength and B is an empirical constant quantifying the wavelength sensitivity. The effective dose, D, describes the degradation caused by exposure to a polychromatic light source, $I(\lambda)$.

Typically light-induced degradation varies linearly with intensity [29] at lower intensities. Because the ceriated and non-ceriated glass adhesion degradation curves are shifted in time by a factor of 8 (Fig. 2), the effective dose, D, should similarly differ by a factor of 8. In the Weather-Ometer® the heat load on the lap shear samples is expected to be nearly identical; therefore, temperature differences would not explain the difference in the rate of adhesion loss between the two glass types. Using $I_{E/G}(\lambda)$ for the different glasses (Eq. (7)), the activation spectra, $E(\lambda)$, for encapsulants behind different front sheet materials were determined (Fig. 5). Integration using Eq. (10) yields values for D for the Ce and non-Ce lap shear samples. Noting that the effective dose, D, differed by a factor of 8 for the two different glasses allowed the wavelength sensitivity to be estimated as B=0.07 (1/nm). This value for the wavelength sensitivity is consistent with that for other polymer systems [33].

The use of an exponential action spectrum has empirical significance, but in the absence of rigorous evaluation [30], it is only a first-order estimate. The effect of different action spectra were evaluated to determine the sensitivity to the assumed profile and to determine the potential range of possible acceleration factors. The simplest action spectrum is that of a step function where all photons below a critical wavelength have equal probability of causing a specified damage (Fig. 6). Assuming the effective dose D differed by a factor of 8 for the 6.35 mm Ce and non-Ce glasses, the critical wavelength for this action spectrum was found to be λ_0=354 nm. However, this model is not a realistic estimation. Furthermore, because the effectiveness of photons does not increase at higher energies, this case most likely represents a lower bound estimate of the accelerated damage caused by increased amounts of UV-B radiation.

A more reasonable action spectrum that accommodates increased damage potential for photons with higher energy is a linear action spectrum. This was estimated with the cut-on wavelength, λ_0, adjusted so that the ratio of effective dose for the

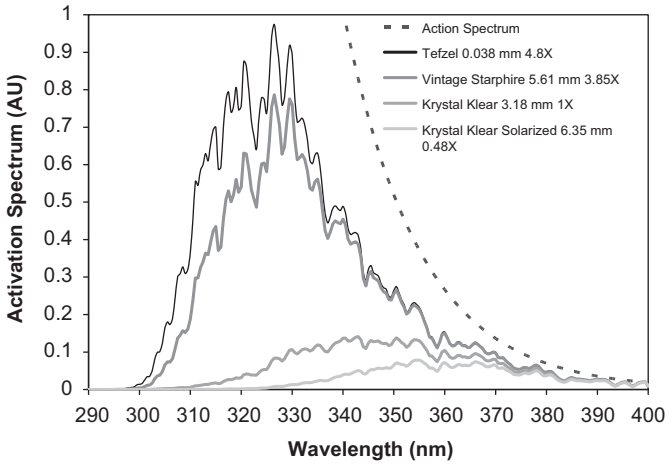

Fig. 5. Activation spectrum showing relative damage potential of light transmitted through different superstrate materials. The relative dose for the different glasses as compared to solarized 3.18 mm Krystal Klear glass is shown in the legend.

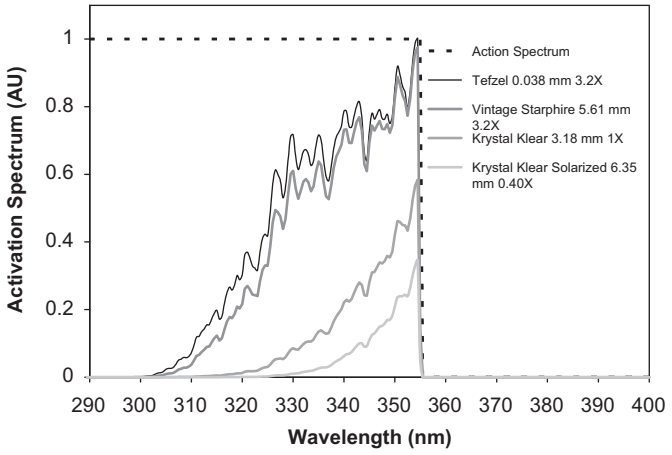

Fig. 6. Activation spectrum constructed using a step function, λ_0=354 nm, for the action spectrum.

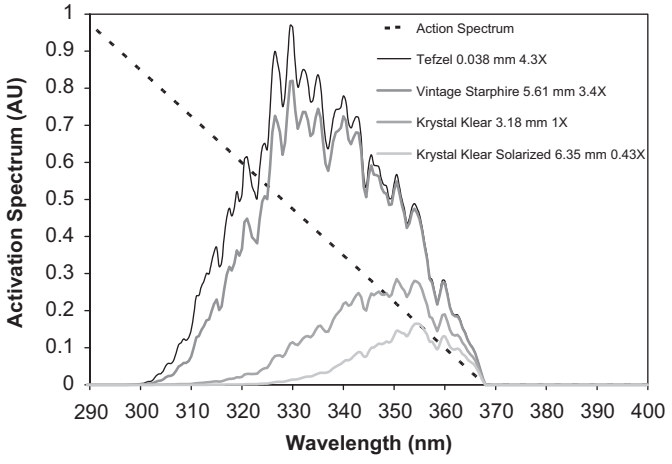

Fig. 7. Activation spectrum constructed using a linear profile for an action spectrum with a cutoff at λ_0=368 nm.

Ce and non-Ce glass lap shear samples would be 8 (see Fig. 7). Using λ_0=368 nm, the activation spectra for different front-sheets were calculated and the acceleration factors relative to 3.18-mm-thick Krystal Klear glass were evaluated. Here it should be noted that the cut-on wavelength for the linear and the step functions do not differ dramatically. All three action spectrum indicate that photons below about 360 nm are the most detrimental to EVA adhesion.

Although significantly different action spectra were used, the UV dose acceleration factors did not vary dramatically (see Table 2). The data for the step function were the most different but it is clear that this result is far from the true action spectrum. Because the differences in the transmittance of the different glasses vary the most at shorter wavelengths, action spectra that emphasize this region (*e.g.* the exponential function) will yield higher acceleration factors than those that emphasize longer wavelengths. Thus the assumed exponential profile for the action spectrum, can be regarded as an upper bound. The true acceleration factors are expected to reside somewhere between the linear results and the exponential function results.

Using 3.18 mm Krystal Klear glass as a reference, the low Fe, non-ceriated PPG Starphire glass transmits UV light that is estimated to cause delamination 3.85 times faster. The environmental chamber irradiates the samples with 2.5 times as much UV radiation as the standard AM 1.5 spectrum. The Weather-Ometer runs 24 hrs a day giving a further UV dose acceleration of approximately 4 for a non-tracking system [10]. This yields a total acceleration factor of 3.85 × 2.5 × 4 = 38.5. Therefore, to obtain a UV dose equivalent to 20 years of exposure, 6.2–7 months of exposure is needed in the Weather-Ometer. However, to get accelerated dose relative to non-Ce, UV transmissive glass, it would take 2 years to get a UV dose equivalent to 20 years.

In Fig. 3 the transmittance of polyethylene-tetrafluoroethylene (ETFE) is shown to illustrate how highly transmissive it is over a wide wavelength region. ETFE is a good candidate for use in flexible PV packaging because of its excellent UV stability and its good anti-soiling properties [31,32]. Because this film is so thin (0.038 mm) there is essentially no absorption in the film and the real component of the refractive index can be estimated from Eqs. (2) and (3) using the transmittance and assuming k=0. This allowed the activation spectrum, Fig. 5, to be calculated using Eqs. (8) and (9). Importantly, this calculation assumes that the wavelength sensitivity for adhesion of EVA to glass is the same as adhesion of EVA to ETFE. If the same silane-based adhesion chemistry that promotes adhesion to glass is a significant factor for the adhesion of EVA to ETFE, this approximation should be reasonable.

When compared to a 3.18-mm-thick Ce-doped glass, ETFE transmits a UV dose that is about 4.8 times more damaging. This is compounded by the fact that fluoropolymers are inherently "non-stick" and difficult to bond to. However, the flexible nature of ETFE relative to glass will allow the packaging to bend to accommodate mechanical stress helping to reduce the interfacial forces promoting deadhesion. If one were to put a ETFE/EVA sample in the Weather-Ometer® at 2.5 UV suns the continuous run duration of 24 h/day will only yield a total acceleration factor of 7.5× for tracking and 10× for non-tracking systems; therefore, to simulate a 20 years UV exposure it will take between 2 and 2.7 years, similar to that for a module constructed using standard non-Ce-doped glass. This illustrates the advantage of using glass substitution to accelerate delamination. It also shows the importance of using a glass doped with Ce (or another UV-B absorber) to maintain good adhesion in service.

3.5. Transmittance loss due to cerium

This high performance of newer EVA formulations has boosted confidence that module performance will be maintained for long

Table 2
Approximate UV dose acceleration factors for different front-sheets.

Action		Exponential B=0.07 (1/nm)	Linear λ_0=368 (nm)	Step λ_0=354 (nm)
Tefzel	0.036 (mm)	5.15	4.44	3.75
Starphire (no Ce)	5.61 (mm)	**4.13**	**3.58**	3.31
Krystal Klear (with Ce)	3.18 (mm)	1	1	1
Krystal Klear (with Ce)	6.35 (mm)	0.51	0.44	0.41

periods of time without significant losses in light transmittance [23,33]. Recently there has been a trend away from the use of Ce-doped glasses in an effort to improve the overall efficiency of solar cells. The removal of Ce from glass not only eliminates some absorption in the UV portion of the spectrum (Fig. 1), but also improves infrared transmittance.

The data in Fig. 1 is for plate glass samples and thus includes effects from reflection at interfaces on both sides of the glass and the absorption for multiple reflections. The amount of light transmittance on one pass to the polymer/glass interface was calculated using Eq. (7) with estimates of the absorptivity of glass as a function of wavelength, $\alpha_{g,\lambda}$. Similarly, the absorptivity of the polymers, $\alpha_{p,\lambda}$, was solved numerically using Eq. (5) and data obtained from samples constructed as 3.18 mm glass/polymer/3.18 mm glass and $\alpha_{g,\lambda}$. With this, the transmittance to the polymer/cell interface was estimated as

$$T_{polymer/cell} = \frac{(1-n_g)^2+k_g^2}{(1-n_g)^2+k_g^2} e^{-(t_g\alpha_{g,\lambda}+t_p\alpha_{p,\lambda})} \quad (11)$$

This approximation does not account for multiple reflections, assumes normal incidence, and ignores reflections at the polymer/glass interface. It represents the maximum amount of light available to a cell.

To facilitate the relative comparison of the performance of different glass/polymer combinations, the transmittance estimates were weighted against the photon density in the solar spectrum and the internal quantum efficiency of a typical monocrystalline silicon cell obtained as an average of cells from 8 different manufacturers, Fig. 8. These QE/solar weighted transmittance measurements are shown in Table 3 for a variety of different glasses from different manufacturers and for EVA and some polydimethyl-siloxane (PDMS)-based polymers.

The use of glass that does not contain Cerium provides an additional 1.4% more photon transmittance to the glass/polymer interface after solarization as compared to a low-Fe Ce-containing glass. Alternatively, glass can be doped with Sb to reduce the absorption of light in the infrared region through enhanced conversion of Fe^{2+} to Fe^{3+}. Unfortunately, Ce cannot be used with Sb because they counteract each other resulting in increased absorption in the infrared region of the spectrum, reducing cell efficiency. However, with antimony alone, an additional 0.1–0.8% photon transmittance can be obtained as compared to non-Ce low-Fe glass. When Ce is removed from glass and replaced with Sb, an additional 1.3–2.2% useable photons will be transmitted through the glass.

PDMS-based encapsulants are naturally stable toward UV radiation and do not require the use of UV absorbers. Therefore they transmit more of the UV light than EVA. However, the number of photons in the UV range is small and the quantum efficiency drops off here also. Despite the fact that 4.6% of the sun's energy is in the UV portion of the spectrum ($\lambda < 400$ nm), the substitution of a silicone for EVA only results in a 0.6–0.7% increase in transmittance. This thorough calculation method

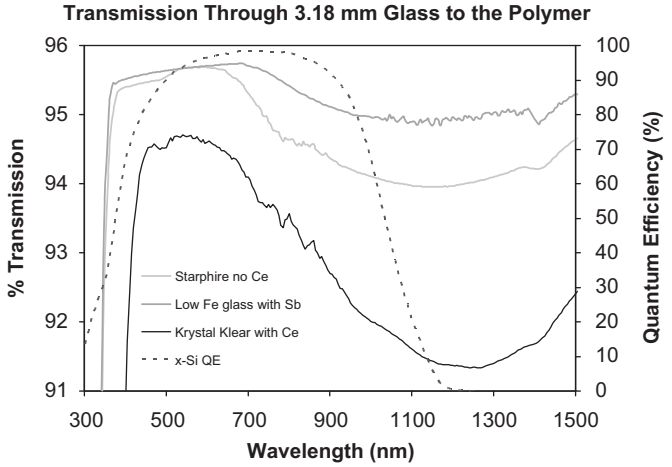

Fig. 8. Percent transmittance of light through 3.18 mm glass to polymer/glass interface and internal quantum efficiency (*x*-Si QE) of a typical monocrystalline silicon PV device.

(Eq. (12)) is consistent with the 0.6% simplified calculation in Table 1 using Eq. (6).

If a Ce-containing glass is replaced with an Sb-containing glass, and EVA is replaced with PDMS, a 1.9–2.9% increase in photon transmittance can be obtained. The substitution of silicone for EVA would be likely to increase encapsulation costs relative to EVA. Because of the high transmittance of silicones, reducing the thickness of PDMS will not improve the optical transmittance significantly, but might reduce the cost of PDMS by half.

Some of the silicones are predicted to outperform EVA by about 0.6% which for a 15% efficient module would result in 0.9 W_p/m^2 more power, which alone might not be sufficient to justify the additional cost for these materials. Similarly a number of other materials with lower transmittance are not sufficiently less expensive than EVA to justify their use. However, EVA is known to produce acetic acid as a by-product [15] and is more polar than silicones and many other polymers. These two factors are likely to produce undesirable effects and may help to justify the use of slightly more expensive encapsulation materials [34–36]. This is more likely to be significant for thin film PV materials, which are more susceptible to corrosion processes [37].

Because of the thinness of the encapsulant layer, the absorption and scattering in EVA only accounts for about a $0.6 \pm 0.2\%$ loss in the potential initial power output of a module. However, EVA will discolor after environmental exposure. The optical transmittance of 0.5-mm-thick aged EVA encapsulant in the lap shear samples was obtained as an estimate of the discoloration of these encapsulants. Following the same procedures for calculating Table 2, it was estimated that EVA and GE RTV 615 [38] would transmit $89.3 \pm 2\%$ and $93.8 \pm 2\%$ after being exposed to 14,364 and 15,238 h, respectively, of 60 °C/60% RH/2.5 UV suns. Similarly, a perfectly transparent encapsulant would transmit 94.8% of the

Table 3
Estimated photon transmittance to a *x*-Si cell behind a 3.18-mm-thick glass and 0.45-mm-thick polymer layer. Transmittance is weighted against the AM 1.5 global solar spectrum and the internal quantum efficiency of a hypothetical typical *x*-Si solar cell obtained from the average of cells from 8 different manufacturers.

Percent transmission to interface:	**Global solar photon and internal quantum effeciency weighted (glass is 3.18 nm thick, polymer is 0.45 mm thick)**								
	Ce glass				Non-Ce glass		Sb glass		PETFE (0.0381 mm thick)
	Unexposed		Solarized		Unexposed	Solarized	#3	#4	
	#1	#2	#1	#2					
Glass sheet transmission	90.3	90.9	89.5	89.3	90.2	90.6	90.8	91.5	94.2
Glass/polymer	94.1	94.8	93.3	93.1	94.7	95.0	94.6	95.4	95.5
EVA/cell	93.4	94.1	92.7	92.5	94.0	94.3	93.9	94.7	94.7
DC 527/cell	94.0	94.7	93.3	93.1	94.7	94.9	94.6	95.4	95.4
GE RTV615/cell	94.1	94.7	93.3	93.1	94.7	95.0	94.6	95.4	95.4

useful photons (QE and AM 1.5 weighted). This represents an additional 5.0% and 0.9% optical loss for EVA and GE RTV 615, respectively, after stress. The small 0.9% transmittance loss for GE RTV 615 is principally due to minor etching and corrosion of the glass. It should also be noted here that this EVA formulation appeared to have more yellowing problems than most.

For a 15% efficient module the 4.7% transmittance difference between aged EVA and RTV 615 would result in an additional 7.1 W_p/m^2 loss. Because 14,000–15,000 h exposure at 60 °C/60% RH/2.5 UV suns produces a greater UV dose than would be experienced over an expected module lifetime, for a module constructed using Ce-containing glass, this should be considered an upper limit for light transmittance losses. One should also consider that oxygen can serve to photobleach a polymer [39], removing the yellow color, and that the ingress of oxygen to enable photobleaching might not be accelerated to the same degree as the UV radiation. As a first-order approximation, the average difference between the performance of an EVA versus a silicone encapsulant would be $(\Delta W_{p,final}+\Delta W_{p,initial})/2=(7.1+0.9)/2=4.0\ W_p/m^2$ loss over the life of a module. The economic value of 4.0 W_p/m^2 gives an upper limit to the benefit associated with a better performing encapsulant. The longer term stability of silicones and other materials may help justify the additional cost of alternative resins and/or better EVA formulations. EVA is the dominant encapsulant used in the PV industry not because it is the best material but because the performance gain from using other encapsulants does not offset their cost.

4. Discussion

Exposure to 6.25 months of UV irradiation at 2.5 UV suns using non-UV blocking glass does not necessarily predict a lifetime of 20 years, but one could be confident that the exposure was of the right order of magnitude. One should also consider that other factors such as thermal cycling, mechanical stress, heat, and humidity also dramatically affect adhesion. For these experiments the choice of 60 °C and 60% RH was somewhat arbitrary but not unreasonably high. Under irradiation in the Weather-Ometer at 60 °C, 60% RH, and 2.5 UV suns, the transparent lap shear samples were found to be at a temperature of 70 °C which means they were actually exposed to about at 38% RH to maintain the same atmospheric absolute humidity. According to prior work by Kempe [39] (see Fig. 4 of that work), the absorption of water by EVA can be modeled as

$$C_{H_2O} = 1.81e^{(-2000/T)} \quad (12)$$

where C_{H_2O} is the concentration of water in EVA in units of g/cm^3 and T is in K. EVA will absorb 0.0020 g/cm^3 moisture at 70 °C and 38% RH which corresponds to saturation of EVA with water at 21.8 °C. Depending on the PV mounting system, location, and time of year, a module will often experience daily maximum temperatures of around 40 °C to 60 °C [40–42] with peaks as high as 70 °C. Therefore, in a hot and humid climate it is possible that portions of a module could saturate with water at low temperatures and then upon heating to 70 °C be exposed to the same temperature and relative humidity of these experiments. According to Ref. [42], a module located in Las Cruces, NM will spend approximately ¼ of its time in the 40–60 °C temperature range. An exposure of 6.25 months at 60 °C, 60% RH with 114 W/m^2 is not an unreasonable exposure and is at the extreme limits of what a module could experience in use for short durations. This avoids conditions of unusually high humidity (*e.g.* 85 °C/ 85% RH) known to dramatically increase corrosion rates [43].

These experiments have demonstrated the strong influence of UV radiation on adhesion. It is found that photon wavelengths below 350 nm are especially damaging with respect to adhesion. Because of this the inclusion of Ce (or other elements that absorb UV-B radiation) in glass is extremely helpful to maintain adhesion [29].

The removal of Ce will increase the UV-induced adhesion degradation by a factor of about 3.8 with only very small additional costs. Additional work is currently being conducted to investigate acceleration factors for transmittance losses in encapsulants. To determine which glass/encapsulant combination is most economical, accurate estimates of light transmittance vs. exposure must be made. Optical performance (enhanced long-term transmissivity) must be weighted against the additional cost of a more robust encapsulant.

5. Conclusions

Materials used for PV encapsulation must be evaluated for their ability to transmit light and to maintain mechanical integrity through extended periods of UV exposure. A survey of candidate encapsulants has indicated that, although the absorptivity can vary greatly, the use of thin encapsulant layers makes absorption differences of secondary importance. Similarly the effects of severe degradation have only a minor effect on light transmittance. Current qualification standards do not adequately evaluate the effects of UV radiation requiring additional tests if one wants to be confident in the longevity of PV modules. Exposure of PV materials to UV radiation in an environmental chamber using highly UV transmissive glass allows UV doses equivalent to 20 years of exposure (relative to stress behind 3.18-mm-thick Ce-doped glass) in about 6 months. This allows reasonable evaluation of PV materials. However, the PV industry has moved away from the use of Ce-containing glass, making the need for such evaluation even more urgent. If one constructed test specimens

with quartz glass rather than low-Fe non-Ce glass then the acceleration factor attributable to glass choice would only be 1.3× as opposed to 3.85× when comparing non-Ce and Ce-containing glass (Table 2). Highly accelerated stress tests like this are necessary to evaluate the effect of UV radiation on module performance. This also highlights the potential risks of using non-Ce-doped glass in PV applications.

Acknowledgments

This work was carried out under US Department of Energy, Contract no. DE-AC36-99G010337. I would like to thank Robert Tirawat, Mike Milbourne, Chris Lundquist, and Andrea Warrick for making sample transmittance measurements. Kent Terwilliger and Marc Oddo for general laboratory help. Keith Emery for providing QE data. And Chris Cording and Mark Spencer for providing glass samples and transmittance spectra.

References

[1] IEC 61215, Crystalline silicon terrestrial photovoltaic (PV) modules—design qualification and type approval.
[2] R.G. Ross, Technology developmentst toward 30-year-life of photovoltaic modules, Proc. 7th IEEE PV Spec. Conf. (1984) 464–472.
[3] IEC 61730-1, Photovoltaic (PV) Module Safety Qualification—Part 1: Requirements for Construction, 2004.
[4] IEC 61730-2, Photovoltaic (PV) Module Safety Qualification—Part 2: Requirements for Testing, 2004.
[5] W.Q. Meeker, L.A. Escobar, Pitfalls of accelerated testing, IEEE Trans. Reliab. 47 (1998) 114–118.
[6] T.J. McMahon, G.J. Jorgensen, R.L. Hulstrom, D.L. King, M.A. Quintana, Module 30 year life: what does it mean and is it predictable/achievable?, in: NCPV Program Review Meeting, Denver, 16–19 April 2000.
[7] IEC 61646, Thin-film terrestrial photovoltaic modules—design qualification and type approval.
[8] IEC 62108, Concentrator photovoltaic (CPV) modules and assemblies—design qualification and type approval.
[9] ASTM G 173-03, Standard tables for reference solar spectral irradiances: direct normal and hemispherical on 37° tilted surface.
[10] L.M. Moore, H.N. Post, Five years of operating experience at a large utility-scale photovoltaic generating plant, Prog. Photovolt.: Res. Appl. 16 (2008) 249–259.
[11] P. Johnson, J. Sites, K. Ramanathan, L. Olsen, D. Tarrant, Effects of buffer layers on SSI CIGSS-absorber transient I–V and C–V behavior, in: 28th IEEE PVSC, Anchorage Alaska, September 2000 17–22.
[12] M. Igalson, C. Platzer-Bjorkman, The influence of buffer layer on the transient behavior of thin film chalcopyrite devices, Sol. Energy Mater. Sol. Cells 84 (2004) 93–103.
[13] H. Hashigami, Y. Itakura, T. Saitoh, Effect of illumination conditions on czochralski-grown silicon solar cell degradation, J. Appl. Phys. 93 (7) (2003) 4240–4245.
[14] M.A. Quintana, D.L. King, T.J. McMahon, C.R. Osterwald, Commonly observed degradation in field-aged photovoltaic modules, in: Proceeding of the 29th IEEE PVSC, New Orleans, 2002.
[15] M.D. Kempe, G.J. Joregensen, K.M. Terwilliger, T.J. McMahon, C.E. Kennedy, T.T. Borek, Acetic acid produciton and glass transitions concerns with ethylene-vinyl acetate used in photovoltaic devices, Sol. Energy Mater. Sol. Cells 91 (2007) 315–329.
[16] ASTM E 313-5, Standard practice for calculating yellowness and whiteness indices from instrumentally measured color coordinates.
[17] ASTM D 1925, Yellowness index of plastics.
[18] D.L. King, M.A. Quintana, J.A. Kratochvil, D.E. Ellibee, B.R. Hansen, Photovoltaic module performance and durability following long-term field exposure, Prog. Photovolt. Res. Appl. 8 (2000) 241.
[19] A. Torikai, H. Hasegawa, Wavelength effect on the accelerated photodegradation of polymethylmethacrylate, Polym. Degradation Stability 61 (1998) 361–364.
[20] H. Xingzhou, Wavength sensitivity of photo-oxidation of polyethylene, Polym. Degradation Stability 55 (1997) 131–134.
[21] X. Hu, Wavelength sensitivity of photo-oxidation of polyamide 6, Polym. Degradation Stability 131–134 (1998) 599–601.
[22] D.E. King, F.J. Pern, J.R. Pitts, C.E. Bingham, A.W. Czanderna, Optical changes in cerium-containing glass as a result of accelerated exposure testing, in: 26th IEEE PVSC, September 29–October 3, Anaheim, California, 1997.
[23] G.U. Zhenan, Spectroscopic properties of doped silica glasses, J. Non-Cryst. Solids 52 (1982) 337–345.
[24] F.J. Pern, S.H. Glick, Improved photostability of NREL developed EVA pottant formulations for PV module encapsulantion, in: 26th IEEE PVSC, September 29–October 3, Anaheim, California, 1997.
[25] W.H. Holley, S.C. Agro, J.P. Galica, L.A. Thoma, R.S. Yorgensen, M. Ezrin, P. Klemchuk, G. Lavigne, H. Thomas, Investigation into the causes of browning in EVA encapsulated flat plate PV modules, in: First WCPEC, December 5–9, Hawaii, 1994.
[26] M. Rubin, Optical properties of soda lime silica glasses, Sol. Energy Mater. 12 (1985) 275–288.
[27] A.L. Andrady, Wavelength sensitivity in polymer photodegradation, Adv. Polym. Sci. 128 (1997) 49–94.
[28] A.L. Andrady, S.H. Hamid, X. Hu, A. Torikai, Effects of increased solar ultraviolet radiation on materials, J. Photochem. Photobiol. B: Biol. 46 (1998) 96–103.
[29] J.R. Pitts, D.E. King, C. Bingham, Ultra accelerated testing of PV module components, in: NCPV Program Review Meeting, Denver, Colorado, September 8–11, 1998.
[30] ASTM G 178-03, Standard practice for determining the activation spectrum of a material (wavelength sensitivity to an exposure source) using the sharp cut-on filter or spectrographic technique.
[31] M. DeBergalis, Fluoropolymer films in the photovoltaic industry, J. Fluorine Chem. 125 (2004) 1255–1257.
[32] E.F. Cuddihy, P.B. Willis, Antisoiling technology: theories of surface soiling and performance of antisoiling surface coatings, DOE/JPL-1012-102 Flat-Plate Solar Array Project (1984).
[33] F.J. Pern, S.H. Glick, Improved photostability of NREL-developed EVA pottant formulations for PV module encapsulation, in: 26th PVSC, September 30–October 3 1997; Anaheim, CA.
[34] M. Vazquez, I. Rey-Stolle, Photovoltaic module reliability model based on field degradation studies, Prog. Photovolt.: Res. Appl.. (2008).
[35] E.D. Dunlop, D. Halton, The performance of crystalline silicon photovoltaic solar modules after 22 years of continuous outdoor exposure, Prog. Photovolt.: Res. Appl. 14 (2006) 53–64.
[36] M.D. Kempe, K.M. Terwilliger, D. Tarrant, Stress induced degradation modes in CIGS mini-modules, in: 33rd IEEE-PVSC, San Diego, CA 2008.
[37] G.R. Mon, R.G. Ross, Electrochemical degradation of amorphous-silicon photovoltaic modules, IEEE (1985) 1142–1149.
[38] This product line was purchased by GE and is now sold by momentive with the same product number
[39] M.D. Kempe, Modeling of rates of moisture ingress into photovoltaic modules, Sol. Energy Mater. Sol. Cells 90 (2006) 2720–2738.
[40] D. Ton, J. Tillerson, T.J. McMahon, M. Quintana, K. Zweibel, Accelerated Aging Tests in Photovoltaics Summary Report, Baltimore, MD, February 22–23 (2006).
[41] D.R. Myers, Predicting temperatures of exposure panels: models and empirical data, Service Life Prediction of Organic Coatings, A Systems Approach, American Chemical Society, Oxford, 1999 (Chapter 6).
[42] T.J. McMahon, Accelerated testing and failure of thin-film PV modules, Prog. Photovolt: Res. Appl. 12 (2004) 235–248.
[43] P. Longrigg, An investigation into the use of inorganic coatings for thin film photovoltaic modules, Sol. Cells 27 (1989) 267–278.